

## Interdecadal Variability of the Relationship between the Indian Ocean Zonal Mode and East African Coastal Rainfall Anomalies

CHRISTINA OELFKE CLARK AND PETER J. WEBSTER

*Program in Atmospheric and Oceanic Sciences, University of Colorado, Boulder, Colorado*

JULIA E. COLE

*Department of Geosciences, The University of Arizona, Tucson, Arizona*

(Manuscript received 27 July 2001, in final form 14 August 2002)

### ABSTRACT

The variance of the rainfall during the October–November–December (OND) “short rain” season along the coast in Kenya and Tanzania correlates strongly with sea surface temperature (SST) in the Indian Ocean between 1950 and 1999. A zonal pattern of positive correlation in the Arabian Sea and negative correlation southwest of Sumatra forms in the summer preceding the rainy season. The positive correlation strengthens in the western Indian Ocean and the negative correlation in the eastern Indian Ocean weakens in the subsequent fall concurrent with the short rain. Reduced OND East African rainfall is associated with the reversed SST pattern. The OND rainfall also correlates strongly with ENSO. The SST–rain correlation pattern breaks down between the years 1983 and 1993, as does the correlation with ENSO. However, between 1994 and 1999 the OND rainfall, ENSO, and the SST zonal mode again return to strong correlation, as in the years preceding 1983.

### 1. Introduction

The East African coast of Kenya and Tanzania (see Fig. 1a for location) experiences two distinct equinoctial rainy seasons, the March–April–May (MAM) “long” rains and the October–November–December (OND) “short” rains, shown in the climatological annual cycle of Fig. 1b. These two rainy seasons do not correlate significantly with each other and are thus relatively independent of each other. Although the highest precipitation occurs during the long rains, the OND season experiences a larger degree of interannual variability relative to climatology (Hastenrath et al. 1993). For example, in 1997, the OND East African rains were in many areas 5–10 times the normal, the highest in the century (World Meteorological Organization 1998). However, in 1996 and 1998 drought conditions persisted. Over the last half century, during the period of reliable rainfall records, the short rains have shown considerable interannual variability. Because of the impact of the short rain variability on agriculture and epidemic and zoonotic diseases, especially malaria and rift-valley fever, predicting the strength of the short rains

with reasonable lead times is of considerable importance.

Several studies have investigated the relationship between the short rains and the El Niño–Southern Oscillation (ENSO). Nicholson and Kim (1997), for example, find a strong connection between ENSO and rainfall over much of the African continent and suggest a linkage through ENSO-induced SST anomalies in the Indian Ocean, which, in turn, modulate interannual variability of rainfall over Africa. An atmospheric general circulation model suggests that the Indian Ocean sea surface temperature (SST) exerts a greater influence over the East African short rains than the Pacific (Goddard and Graham 1999).

Empirical studies find that the short rains correlate strongly with SST in the western Indian Ocean (Mutai et al. 1998; Nicholson 1997; Ogallo et al. 1988; Cadet and Diehl 1984), suggesting that Indian Ocean SST is a major contributor to the variability of the short rains. A potential candidate for short rain variability is the Indian Ocean zonal mode (IOZM), sometimes referred to as the Indian Ocean dipole (Saji et al. 1999; Yu and Rienecker 1999, 2000). We prefer to use the term IOZM as it matches the out-of-phase development of the SST extrema in the east and west Indian Ocean, consistent with the physics suggested by Webster et al. (1999). The term dipole, on the other hand, suggests simultaneous variation in the east and west. The positive IOZM is

---

*Corresponding author address:* Christina Clark, Program in Atmospheric and Oceanic Sciences, University of Colorado, Campus Box 311, Boulder, CO 80309–0311.  
E-mail: oelfke@bogat.colorado.edu

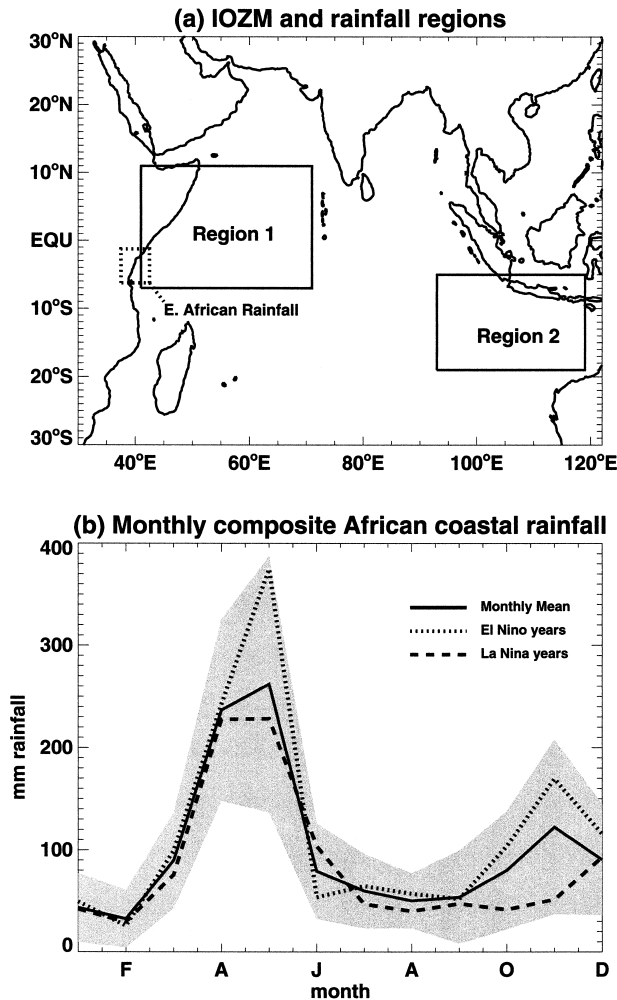


FIG. 1. (a) Map of the Indian Ocean area indicating the region of the East African rainfall (box within dotted line), the NW node of the IOZM (region 1), and the SE node (region 2). (b) Composites of African rainfall showing the monthly mean (solid line), monthly composites for El Niño years (dotted line), and monthly composites for La Niña years (dashed line). The shaded region indicates the monthly mean plus and minus one std dev.

characterized by a reversal of the east–west equatorial gradient in SST across the Indian Ocean, with warmer than normal water along the equatorial east coast of Africa and cool water near Sumatra. The negative anomalies in the east tend to lead the positive western anomalies by one season. The negative IOZM is characterized by reversed anomalies. This mode appears to have a complicated relationship with ENSO, occurring at times of ENSO extrema and at other times when the Pacific Ocean was not anomalous (Reason et al. 2000; Webster et al. 1999; Saji et al. 1999).

Simultaneous with the strong El Niño event of 1997/98, an extreme example of a positive IOZM event occurred during the early boreal fall of 1997 when strong upwelling and cooling occurred along the Sumatra coast. Later in the year, as the cold waters in the eastern

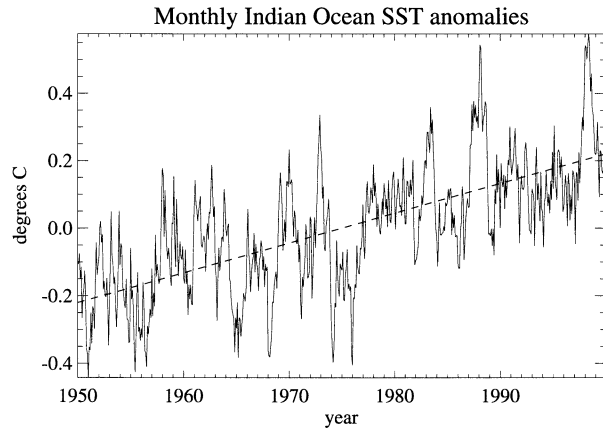


FIG. 2. Time series of anomalous Reynolds SST averaged over the tropical Indian Ocean ( $31^{\circ}\text{S}$ – $31^{\circ}\text{N}$ ,  $37^{\circ}$ – $131^{\circ}\text{E}$ ). The dashed line is a linear least squares fit from 1950 to 1999 with a slope of  $0.009^{\circ}\text{C yr}^{-1}$ .

Indian Ocean warmed, strong warming occurred in the western Indian Ocean, maintaining the SST differential between the western and eastern Indian Ocean. Throughout the entire period the SST gradient along the equator was reversed. Webster et al. (1999) showed the sequence of events to be a coupled ocean–atmosphere instability that perpetuated the longitudinal SST gradient. This SST zonal gradient has appeared many times during the last few decades (Webster et al. 1999; Saji et al. 1999; Reverdin et al. 1986), although with a smaller magnitude than occurred in 1997. In recent decades, only in 1961 did the IOZM have a similar amplitude to 1997. Webster et al. (1999) speculated that this mode was responsible for the devastating 1997–98 floods in East Africa.

Analysis of long-term data shows that the monthly tropical Indian Ocean SST correlates with the Niño-3 ( $5^{\circ}\text{S}$ – $5^{\circ}\text{N}$ ,  $90^{\circ}$ – $150^{\circ}\text{W}$ ) Pacific SST index at +0.4 (Clark et al. 2000; Turre and White 1995), and with the Niño-3.4 ( $5^{\circ}\text{S}$ – $5^{\circ}\text{N}$ ,  $120^{\circ}$ – $170^{\circ}\text{W}$ ) index at +0.65 simultaneously, and +0.75 when Niño-3.4 leads by 3 months (Fig. 1 in Goddard and Graham 1999). El Niño (La Niña) events tend to be accompanied by anomalously high (low) SST in the Indian Ocean. After 1976, more El Niño and fewer La Niña events occurred than previously, seemingly in conjunction with a shift to a warmer state in the tropical oceans (Trenberth and Hoar 1996; Trenberth 1990). Since 1945 the Indian Ocean has experienced an average warming trend of  $0.01^{\circ}\text{C yr}^{-1}$  (Clark et al. 2000; Terray 1994) with a  $0.3^{\circ}\text{C}$  shift to a warmer state that occurred around 1976, in parallel with the other tropical oceans (Wang 1995; Trenberth 1990; Graham 1994; Terray 1994). The warming trend and the 1976 SST shift are clearly visible in the time series of monthly anomalies of the Reynolds SST (described in the data section) averaged over the tropical Indian Ocean (Fig. 2). After 1976 there are no strong negative SST anomalies, below  $-0.12^{\circ}\text{C}$ . As the East African short

rains are clearly linked to Indian Ocean SST anomalies, it is important to identify the influence of the Indian Ocean warming trend and the 1976 shift on the interdecadal variability of the short rains.

The purpose of this paper is to further explore the ways in which the Indian Ocean can influence the East African short rains in conjunction with (and independently of) ENSO, and the interdecadal variability of the SST–ENSO–rainfall relationships.

## 2. Data

The SST data used in this study are the monthly Reynolds reconstructed SST (Smith et al. 1996) on a  $4^\circ \times 4^\circ$  grid spanning the tropical Indian Ocean ( $31^\circ\text{S}$ – $31^\circ\text{N}$ ,  $37^\circ$ – $131^\circ\text{E}$ ) from 1950 to 1999. The Niño-3.4 SST index represents the strength of ENSO and is computed from the average Reynolds SST anomalies over the central equatorial Pacific ( $5^\circ\text{S}$ – $5^\circ\text{N}$ ,  $120^\circ$ – $170^\circ\text{W}$ ).

Monthly precipitation data from six coastal stations (Lamu, Mombasa, Tanga, Zanzibar, Pangani, and Dar es Salaam, Africa) for the years 1945–94 were provided by S. Nicholson (The Florida State University, 1999, personal communication). The rainfall stations are located within the box labeled “E. African Rainfall” in Fig. 1a. These data are supplemented for more recent years (1995–99) by the monthly Climate Prediction Center (CPC) Merged Analysis of Precipitation [CMAP; Xie and Arkin 1996; data available from the National Oceanic and Atmospheric Administration (NOAA)–CPC data center], available for the years 1979–99, averaged over roughly the same area as the station data. From 1979 to 1994, when the two precipitation datasets overlap, the two OND average rainy season datasets correlate at +0.78. It is clear in Fig. 1a that the African rainfall is measured over a very small area. However, between 1979 and 1999 the CMAP precipitation from the small region correlates with precipitation averaged over a larger region (a  $25^\circ \times 25^\circ$  box over the range  $11.25^\circ\text{S}$ – $13.75^\circ\text{N}$ ,  $25^\circ$ – $50^\circ\text{E}$ ) at a value of 0.90. Thus, within the limitations of the CMAP data, OND rainfall from the small region from which the station data are available are representative of a larger region of the East African equatorial coast including the greater Horn of Africa region.

## 3. Results

We examine the monthly average variation of the East African coastal rainfall. The shaded region of Fig. 1b denotes the variance of the rainfall, the mean plus and minus one standard deviation. Clearly visible are the MAM and OND rainy seasons, with the long rains having nearly twice the amplitude of the short rains. Also shown are the monthly composite rainfall for El Niño years (dotted line: years 1957, 1965, 1972, 1982, 1986, 1987, 1991, 1994) and for La Niña years (dashed line: years 1955, 1964, 1970, 1973, 1975, 1988). El Niño

years are defined as years in which the OND Niño-3.4 index is more than one standard deviation above the mean, and La Niña years are years in which the OND Niño-3.4 is more than one standard deviation below the mean. The occurrence of El Niño tends to enhance the OND rainfall, while La Niña tends to diminish it. Overall, considerable variability in East African rainfall is accounted for by ENSO. From 1950 to 1999 the OND East African rainfall correlates with the OND Niño-3.4 SST index at +0.55; thus, ENSO accounts for approximately 30% of the variance of the OND rainfall.

Figures 3a–c show the correlations between seasonal Reynolds SST with the OND East African short rains defined in the last section. Significance levels are calculated using a two-tailed Student's *t* test. The analysis reveals a strong zonal pattern of positive correlations in the western Indian Ocean and negative correlations near Indonesia in the summer preceding the rainy season when calculated for the years 1950–82 (Fig. 3b). The analysis is in general agreement with Nicholson (1997). The region of positive correlation expands in the fall season concurrent with the short rains, while the negative correlation region is reduced (Fig. 3c).

We chose to emphasize in Figs. 3a–c the time period 1950–82 because it yielded the highest correlations compared with later periods. When the same correlation analysis is done for the period from 1983 to 1993, the results differ significantly (Figs. 3d–f). During this period the correlation pattern is nearly reversed in sign, with negative correlations in the western Indian Ocean in the spring and summer, and positive correlation in the southeastern Indian Ocean in the summer and fall seasons. We exclude the years 1994–99 from this time period because strong positive IOZM events occurred in 1994 and 1997 (Webster et al. 1999) accompanied by strong OND precipitation anomalies. Additionally, there were strong negative IOZM events in 1996 and 1998 with negative rainfall anomalies. If the 1994–99 data are included in the analysis shown in Figs. 3d–f (i.e., 1983–99) the fields of SST correlations are very similar to those of Figs. 3a–c. However, we exclude these years to emphasize the changes in patterns occurring in the 1983–93 period.

In Fig. 3b, during the period 1950–82, the maximum correlations between rainfall and SST are +0.53 in the western Indian Ocean and –0.46 in the eastern Indian Ocean for July–August–September (JAS). In OND, these patterns extend to a much broader region correlated at +0.72 in the western Indian Ocean, but the negative correlations fall to –0.3 in the east (Fig. 3c). These correlation patterns match the evolution of the IOZM described earlier, in which negative SST anomalies in the eastern Indian Ocean precede positive anomalies in the western Indian Ocean, and die off earlier (Saji et al. 1999; Webster et al. 1999).

Strong correlations of rainfall with SST leading by one season would suggest the potential for empirical prediction of the short rains. However, any empirical

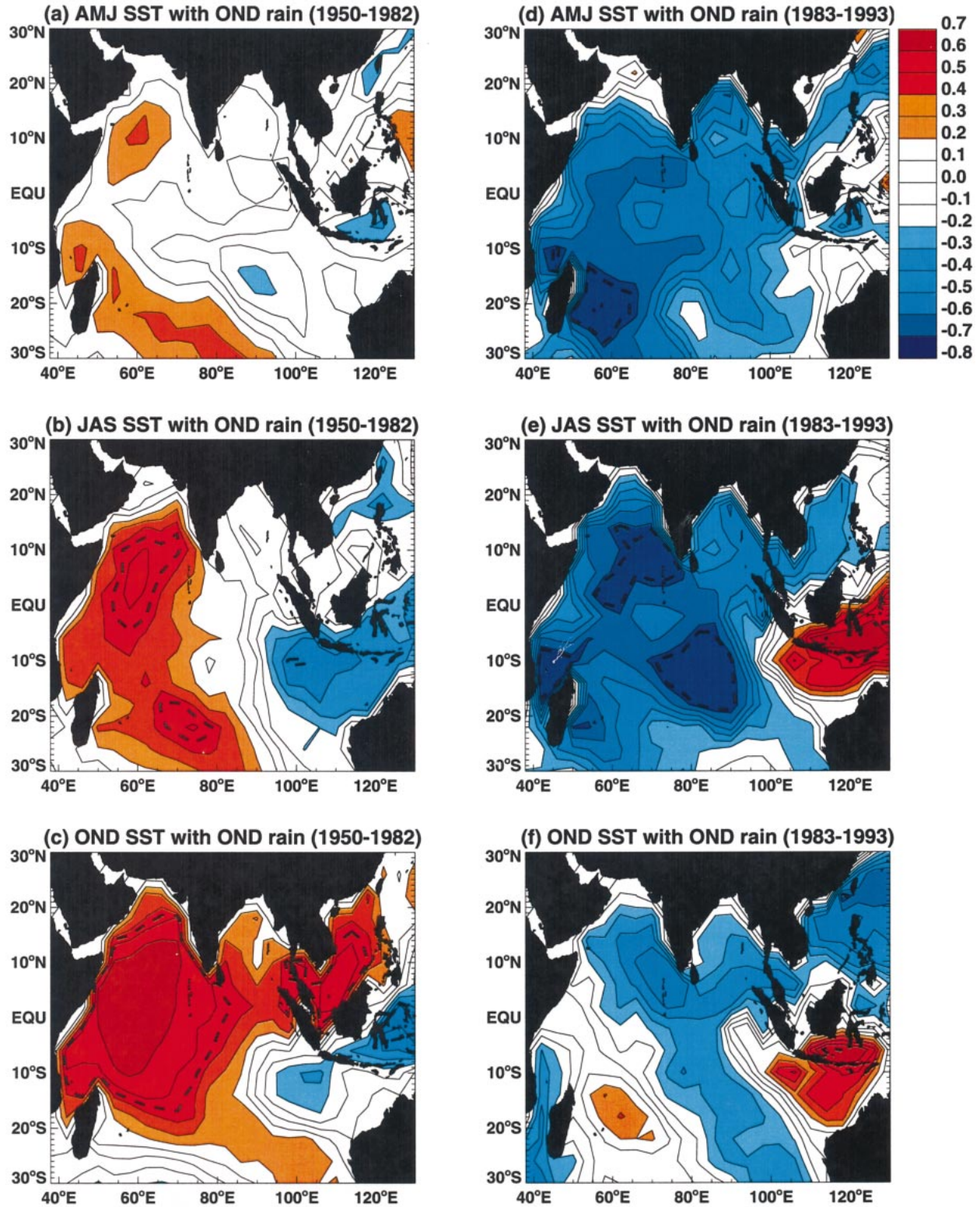


FIG. 3. Seasonal correlations of Indian Ocean Reynolds SST with the OND East African rain for (a), (b), (c) the years 1950–82, and (d), (e), (f) the years 1983–93. Bold, dashed lines indicate the 99% significance level [0.45 for (a), (b), (c); 0.73 for (d), (e), (f)].

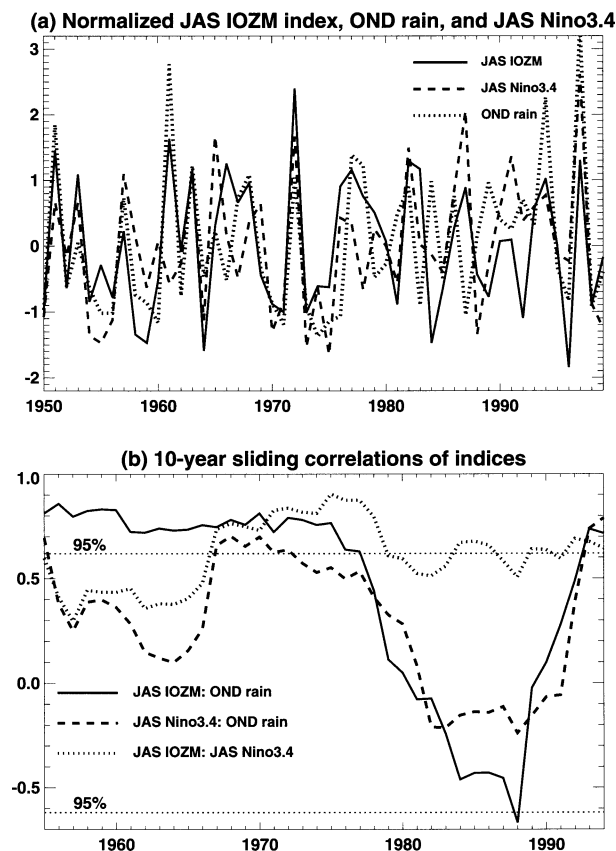


FIG. 4. (a) Time series of the normalized JAS IOZM index (solid line), the OND East African rainfall (dotted line), and the JAS Niño-3.4 index (dashed line). (b) Sliding correlations with a 10-yr window between the JAS IOZM and the OND rain (solid line), the JAS Niño-3.4 and the OND rain (dashed line), and the JAS IOZM and the JAS Niño-3.4 (dotted line). The horizontal dotted lines indicate the 95% significance level ( $\pm 0.63$ ).

predictive scheme depends on the stability of the empirical relationships over time. We define an IOZM index composed of JAS SST averaged over the strongest positive correlation region in Fig. 3b ( $7^{\circ}\text{S}$ – $11^{\circ}\text{N}$ ,  $41^{\circ}$ – $71^{\circ}\text{E}$ , region 1 in Fig. 1a) minus the SST averaged over the negative correlation region ( $19^{\circ}$ – $5^{\circ}\text{S}$ ,  $93^{\circ}$ – $119^{\circ}\text{E}$ , region 2 in Fig. 1a). This index is plotted with the OND

East African rainfall (Fig. 4a). Clearly, the JAS IOZM index (solid line) correlates more strongly with the OND rainfall (dotted line) between 1950 and 1982, after which time they decorrelate, before regaining correlation from 1994 to 1999. Also plotted in Fig. 4a is the JAS Niño-3.4 SST anomaly (dashed line).

Sliding correlations with a 10-yr window between the JAS IOZM index, JAS Niño-3.4, and the OND rainfall illustrate the large interdecadal changes in correlations (Fig. 4b). The horizontal dashed lines indicate the 95% significance level for a two-tailed Student's  $t$  distribution. The correlation of the JAS IOZM with the OND rainfall is positive and significant through the mid-1970s before dropping sharply to negative values during the 1980s and reaching significant negative values in 1988. At the same time, the correlation of the Niño-3.4 with the rainfall also drops, while the correlation between the IOZM with Niño-3.4 remains strong.

To determine these interdecadal variations in more detail, correlation coefficients between the different indices for various time periods were calculated and are shown in Table 1. We include both the OND and JAS seasons for Niño-3.4 and the IOZM SST indices, as well as each node of the IOZM (regions 1 and 2 in Fig. 1a). We have not computed correlation coefficients exclusively for the 1994–99 period because of a lack of statistical significance, but clearly a strong ENSO–IOZM–rainfall relationship exists during this time (see Fig. 4a). This is especially visible in 1997, when strong OND rainfall occurred simultaneously with a very strong positive IOZM event and an El Niño event (Webster et al. 1999; Saji et al. 1999).

Between 1950 and 1982 the correlation of the JAS and OND IOZM with the OND East African rainfall is 0.73 and 0.76, respectively. Between 1983 and 1994 this correlation drops to  $-0.66$  and  $-0.29$ , respectively. The western node of the IOZM is primarily responsible for this change, as it shifts from positive to negative values (the correlation of JAS and OND western node SST with rainfall shifts from 0.57 and 0.69, to  $-0.72$  and  $-0.23$ , respectively).

The relationship between JAS and OND Niño-3.4 and the OND rainfall also drops to insignificant values after

TABLE 1. Correlations between OND East African rainfall (A), JAS Niño-3.4 (B), OND Niño-3.4 (C), and Indian Ocean SST indices (D–I) for the following years: 1950–82, 1983–93, and 1950–99.

Index	1950–82 index			1983–93 index			1950–99 index		
	A	B	C	A	B	C	A	B	C
A. OND rainfall	1.0			1.0			1.0		
B. JAS Niño-3.4	0.48	1.0		$-0.24$	1.0		0.50	1.0	
C. OND Niño-3.4	0.54	0.95	1.0	$-0.04$	0.91	1.0	0.55	0.94	1.0
D. JAS IOZM	0.73	0.66	0.62	$-0.66$	0.51	0.39	0.56	0.61	0.59
E. OND IOZM	0.76	0.71	0.72	$-0.29$	0.72	0.75	0.64	0.71	0.73
F. JAS western node	0.57	0.50	0.49	$-0.72$	0.18	$-0.04$	0.39	0.48	0.36
G. OND western node	0.69	0.71	0.73	$-0.23$	0.58	0.55	0.63	0.71	0.66
H. JAS eastern node	$-0.46$	$-0.43$	$-0.39$	0.11	$-0.48$	$-0.55$	$-0.30$	$-0.27$	$-0.36$
I. OND eastern node	$-0.16$	$-0.06$	$-0.05$	0.22	$-0.54$	$-0.60$	$-0.07$	$-0.08$	$-0.16$

1983 (correlation changing from 0.48 and 0.54, to  $-0.24$  and  $-0.04$ , respectively). However, the correlations between the IOZM and index with Niño-3.4 remain relatively constant throughout the entire 50-yr period of analysis.

#### 4. Discussion and conclusions

This study demonstrates that there are strong correlations between Indian Ocean SST and East African short rains, but that there was a significant change in this relationship between 1983 and 1993. Other studies (Mutai et al. 1998; Ogallo et al. 1988; Nicholson and Entekhabi 1987) have found SST patterns in the 1950–82 period that are associated with the short rains. Some of these hint at a SE–NW pattern (e.g., Mutai et al. 1998, their Fig. 2) similar to what we have found for the same period. We ascribe the pattern to a reoccurring coupled ocean–atmosphere mode (the IOZM) as described by Webster et al. (1999). The SST pattern strongly correlated with the OND East African rainfall resembles the dipole mode described by Saji et al. (1999). Although the IOZM index described in this paper is not independent of ENSO, it is more strongly correlated with the East African short rains than the Niño-3.4 index is.

Between 1983 and 1993 we find that correlations between SST and precipitation nearly reverse in sign. Additionally, the correlation between OND rainfall and the Niño-3.4 index weakens between 1983 and 1993. The factors causing this change are beyond the scope of this study, but this decade can at least be described as having less variance in the OND rainfall, JAS IOZM, and JAS Niño-3 index than in years before or since (see Fig. 4a). Perhaps in the absence of IOZM or ENSO extremes, other factors, such as climate processes over Africa, dominate the variability of the East African short rains. Additionally, several studies identify a change in the evolution of ENSO simultaneous with a shift to a warmer state in Indian Ocean SST in 1976 (Clark et al. 2000; Wang 1995; Graham 1994; Trenberth 1990; see Fig. 2 of this paper). Although the change in the OND rainfall–IOZM relationship occurred seven years later, there may be a connection between this warming shift and the interdecadal variability of precipitation over Africa.

Interestingly, from 1994 to 1999 the IOZM index, OND rainfall, and the Niño-3.4 index are very strongly correlated, similar to the regime before 1983. Between 1994 and 1999 there have been a sequence of negative and positive dipole events with roughly a 2-yr period accompanied by OND East African rainfall anomalies as seen in the epoch before 1983. It would thus appear that the current interaction of Indian Ocean SST with African rainfall may be similar to the epoch between 1945 and 1982.

Clearly, the dynamics governing the relationship between Indian Ocean SST and the East African short rains varies interdecadally. The high correlation of JAS Indian

Ocean SST (the positive phase of the IOZM before 1983 and after 1993, and the negative phase between these years, see Table 1) with OND East African rainfall suggests the potential for rainfall prediction. However, a better understanding of the cause of the interdecadal variations is needed before improved long-lead empirical forecasting of precipitation can be achieved.

*Acknowledgments.* This research was supported by the National Science Foundation Grants ATM-9526030, ATM-9985557, OCE-0096319, and OCE-9614137. Thank you to Dr. Sharon Nicholson and Doug Klotter for African rain gauge data. Special thanks to Balaji Ragagopalan, W. Han, and K. Sahami for discussions.

#### REFERENCES

- Cadet, D. L., and B. Diehl, 1984: Interannual variability of the surface field over the Indian Ocean during the recent decades. *Mon. Wea. Rev.*, **112**, 21–25.
- Clark, C. O., J. E. Cole, and P. J. Webster, 2000: Indian Ocean SST and Indian summer rainfall: Predictive relationships and their decadal variability. *J. Climate*, **13**, 2503–2519.
- Goddard, L., and N. E. Graham, 1999: Importance of the Indian Ocean for simulating rainfall anomalies over eastern and southern Africa. *J. Geophys. Res.*, **104**, 19 099–19 116.
- Graham, N. E., 1994: Decadal-scale climate variability in the tropical and North Pacific during the 1970s and 1980s: Observations and model results. *Climate Dyn.*, **10**, 135–162.
- Hastenrath, S., A. Nicklis, and L. Greischar, 1993: Atmospheric–hydrospheric mechanisms of climate anomalies in the western equatorial Indian Ocean. *J. Geophys. Res.*, **98**, 20 219–20 235.
- Mutai, C. C., M. N. Ward, and A. W. Colman, 1998: Towards the prediction to the East Africa short rains based on sea surface temperature–atmosphere coupling. *Int. J. Climatol.*, **18**, 975–997.
- Nicholson, S. E., 1997: An analysis of the ENSO signal in the tropical Atlantic and western Indian Oceans. *Int. J. Climatol.*, **17**, 345–375.
- , and D. Entekhabi, 1987: Rainfall variability in equatorial and southern Africa: Relationships with sea surface temperatures along the southwestern coast of Africa. *J. Climate Appl. Meteor.*, **26**, 561–578.
- , and J. Kim, 1997: The relationship of the El Niño–Southern Oscillation to African rainfall. *Int. J. Climatol.*, **17**, 117–135.
- Ogallo, L. J., J. E. Janowiak, and M. S. Halpert, 1988: Teleconnection between seasonal rainfall over East Africa and global sea surface temperature anomalies. *J. Meteor. Soc. Japan*, **66**, 807–821.
- Reason, C. J. C., R. J. Allan, J. A. Lindesay, and T. J. Ansell, 2000: ENSO and climatic signals across the Indian Ocean basin in the global context. Part I: Interannual composite patterns. *Int. J. Climatol.*, **20**, 1285–1327.
- Reverdin, G., D. L. Cadet, and D. Gutzler, 1986: Interannual displacements of convection and surface circulation over the equatorial Indian Ocean. *Quart. J. Roy. Meteor. Soc.*, **112**, 43–67.
- Saji, N. H., B. N. Goswami, P. N. Vinayachandran, and T. Yamagata, 1999: A dipole mode in the tropical Indian Ocean. *Nature*, **401**, 360–363.
- Smith, T. M., R. W. Reynolds, R. E. Livezey, and D. C. Stokes, 1996: Reconstruction of historical sea surface temperature using empirical orthogonal functions. *J. Climate*, **9**, 1403–1420.
- Terray, P., 1994: An evaluation of climatological data in the Indian Ocean area. *J. Meteor. Soc. Japan*, **72**, 359–386.
- Trenberth, K. E., 1990: Recent observed interdecadal climate changes in the Northern Hemisphere. *Bull. Amer. Meteor. Soc.*, **71**, 988–993.
- , and T. J. Hoar, 1996: The 1990–1995 El Niño–Southern Os-

- cillation event: Longest on record. *Geophys. Res. Lett.*, **23**, 57–60.
- Tourre, Y. M., and W. B. White, 1995: ENSO signals in global upper-ocean temperature. *J. Phys. Oceanogr.*, **25**, 1317–1332.
- Wang, B., 1995: Interdecadal changes in El Niño onset in the last four decades. *J. Climate*, **8**, 267–285.
- Webster, P. J., A. M. Moore, J. P. Loschnigg, and R. R. Leben, 1999: Coupled ocean–atmosphere dynamics in the Indian Ocean during 1997–1998. *Nature*, **401**, 356–360.
- World Meteorological Organization, 1998: WMO statement on the status of the global climate in 1997. WMO Tech. Doc. 877, 12 pp.
- Xie, P., and P. A. Arkin, 1996: Analyses of global monthly precipitation using gauge observations, satellite estimates, and numerical model predictions. *J. Climate*, **9**, 840–858.
- Yu, L. S., and M. M. Rienecker, 1999: Mechanisms for the Indian Ocean warming during the 1997–1998 El Niño. *Geophys. Res. Lett.*, **26**, 735–738.
- , and —, 2000: Indian Ocean warming of 1997–1998. *J. Geophys. Res.*, **105**, 16 923–16 939.